The Microtube Strip Heat Exchanger

F. DAVID DOTY, GREG HOSFORD, and J. B. SPITZMESSER

Doty Scientific, Inc., Columbia, South Carolina 29223

JOHN DEWEY JONES

Associate Professor, School of Engineering Science, Simon Fraser University, Burnaby, British Columbia V5A 1S6

The advantages of designing heat exchangers in the laminar-flow regime are discussed from a theoretical standpoint. It is argued that laminar-flow designs have the advantages of reducing thermodynamic and hydrodynamic irreversibilities, and hence increasing system efficiency. More concretely, laminar-flow heat exchangers are free from the turbulence-induced vibration common in conventional heat exchangers, and can thus offer longer life and greater reliability.

The problems of manufacturing heat exchangers suited to laminar flow are discussed. A method of manufacture is outlined that allows compact, modular design. Experience with this method of manufacture is described. Experimental results with a prototype heat exchanger bank are presented; these results show good agreement with theory at moderate levels of effectiveness (75–85%), but fall below predicted values at higher levels. It is argued that this discrepancy results from flow maldistribution. The problems of fouling and flow maldistribution are briefly discussed, and some possible applications are mentioned.

INTRODUCTION

Heat exchanger design always involves a compromise among three objectives: maximizing the heat exchanger effectiveness; minimizing the work required to overcome fluid friction in the heat exchanger; and minimizing the manufacturing and material costs of the exchanger. In the past, the third objective has pushed design in the direction of high-turbulence heat exchangers, to take advantage of the high heat transfer coefficient associated with turbulent flow. But with respect to the first two objectives this is a poor choice: Turbulent flow exacts a disproportionately high penalty in pumping work, and the vibration engendered by turbulence shortens the life of the equipment. Second-law analysis shows us that high-efficiency heat exchangers must be nonturbulent, with minimum temperature difference between counterflowing streams [1].

By taking advantage of modern manufacturing techniques, we can produce heat exchanger designs that would have been impossible at the time that current design practices evolved. This allows us to seek greater reliability and higher efficiency by exploring designs that operate in the laminar-flow regime. In the following paragraphs we establish some of the basic design principles that hold in that regime. Our first interest is in gas-to-gas heat exchangers, though some of our remarks will also apply to liquid–gas and liquid–liquid heat exchange.

It will be shown that it is desirable to operate at very high static pressures (1 to 5 MPa) to minimize

We would like to thank David Gordon Wilson of the Department of Mechanical Engineering at MIT, who made several helpful suggestions for modification of an earlier draft of this article. We would also like to thank the anonymous reviewers, whose comments have led us to think more deeply on many of the topics we discuss. The deficiencies that remain in the article are, of course, the responsibility of the authors.

the flow velocity. Mechanical stress considerations therefore favor a tubular design.

Current practice in compact heat exchangers is dominated by crossflow designs because they are thought to simplify manifolding problems. However, crossflow has a maximum practical effectiveness of 80% for symmetric flow conditions, and pumping power losses are increased due to unavoidable turbulence. Several crossflow exchangers may be used in series to achieve higher effectiveness, but a counterflow exchanger is the only practical method of approaching 100% effectiveness under symmetric flow.

A counterflow heat exchanger module is shown in Fig. 1. It consists of a large number of small tubes, manifolded together in parallel, with a surrounding cage to establish counterflow conditions. Counterflow exchangers have been used for decades to achieve very high heat recovery [2]. In theory it has never been difficult to achieve 95% effectiveness, but aside from cryogenic applications this requires prohibitively large and expensive exchangers for gases. We find that a 95% effective heat exchanger currently costs at least eight times as much as a 60% effective design.

For large-scale production of heat exchangers, as for most other goods produced on a sufficiently large scale, the dominant cost is that of the raw materials used [3]. This is especially true when novel manufacturing techniques allow a significant reduction in manufacturing costs. For this reason, power density or specific conductance (defined as UA/m_S W/kg K, where m_S is the total heat exchanger mass) is one of the most significant figures of merit for a heat exchanger. We show later how this figure can be maximized for a laminar counterflow heat exchanger, while keeping the pressure drop and axial conduction losses within reasonable bounds. We then test this analysis against experiment. In summary, our analysis shows that we should reduce tube diameter to the smallest value it is feasible to manufacture, keeping pressure drop in check by shortening the tubes, increasing their number, and perhaps increasing the operating pressure.

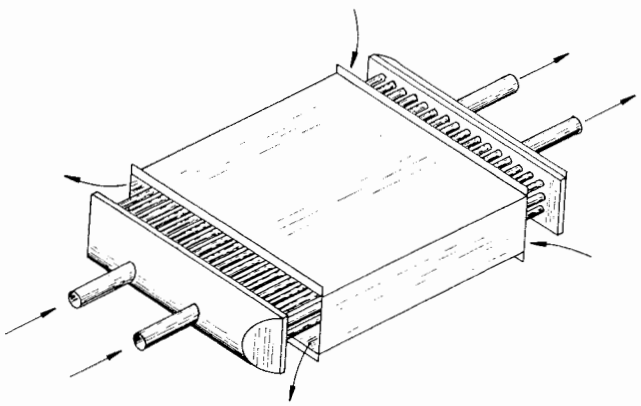

Figure 1 An MTS module.

THEORETICAL ANALYSIS OF LAMINAR-FLOW HEAT EXCHANGERS

Heat exchangers are generally evaluated in terms of their *effectiveness*, ϵ, where effectiveness is defined as the ratio of heat actually transferred to that which would be transferred by a heat exchanger having infinite heat transfer area and operating under the same conditions. It may be shown that for a counterflow heat exchanger exchanging heat between two fluid streams, mass flow rates $\dot{m}_C$ and $\dot{m}_H$, specific heats c_C and c_H, the effectiveness is given by [4]

$$\epsilon = \frac{1 - e^{-\mathrm{NTU}(1-R)}}{1 - e^{-\mathrm{NTU}(1-R)}R} \tag{1}$$

where NTU denotes the number of transfer units:

$$\mathrm{NTU} = \frac{UA}{c\dot{m}} \tag{2}$$

c and $\dot{m}$ being the specific heat and mass flow rate of the fluid stream having the lesser heat capacity, and where R denotes the ratio of the lesser heat capacity to the greater:

$$R = \frac{c_{\min}\dot{m}_{\min}}{c_{\max}\dot{m}_{\max}} \tag{3}$$

If the capacities of the two streams are equal, the right-hand side of Eq. 1 becomes undefined and must be replaced by the simpler expression,

$$\epsilon = \frac{\mathrm{NTU}}{\mathrm{NTU} + 1} \tag{4}$$

For laminar-flow conditions, it is well known that the heat-exchange capacity of a tube of given length is independent of tube diameter and gas velocity. (See, for example, Problem 14c on p. 108 of [5].) The independence of Nusselt number, Nu, from Reynolds number, Re, for laminar flow indicates that heat transfer between tube side and shell side is determined solely by the two fluid conductivities and geometric factors.

Consider a tubular counterflow heat exchanger made up of n tubes, length L, internal diameter d_i, with laminar flow within and without. We shall assume that the fluid flowing within the tubes is the hotter on entry. We may take the conductivity of the tube material to be large compared with that of the two fluids, and hence write

$$UA = 4\pi nL\left(\frac{k_C k_H}{ak_C + bk_H}\right) \tag{5}$$

where k_H and k_C are the thermal conductivities of the inner and outer gases, respectively, and a and b are dimensionless coefficients of the order of unity that are functions of tube inner and outer diameters and tube spacing. (It is acknowledged that the use of thermal conductivities instead of heat transfer coefficients is unconventional; we claim, however, that it correctly represents the relevant physical dependencies, and that it may reasonably be used to establish a qualitative design strategy.) For tube centers spaced $2d_i$, with tube wall $w = 0.2d_i$, a is approximately 0.7 and b is unity. We shall assume these geometric relationships and take $k_C = k_H$ for the remainder of this discussion.

In addition to achieving a certain effectiveness, the designer will be concerned with the cost of the heat exchanger, the pumping losses, and conduction losses. We shall also insist that the flow remains laminar. Constraints can be written down corresponding to these requirements. In the following paragraphs we shall develop the constraints for the tube-side flow; the arguments for shell-side flow are very similar.

In conventional heat exchanger design, machining and assembly costs overshadow the cost of the materials used. However, for reasons to be explained later, we shall consider material costs as primary. The mass of material required for the microtubes in a heat exchanger is then

$$M = 0.24\pi d_i^2 nL\rho_m \tag{6}$$

The tube-side pumping power loss $\dot{W}_p$ can be expressed in terms of the tube-side mass flow rate $\dot{m}_H$ as follows [6]:

$$\Delta p = \frac{128\mu L\dot{m}_H}{\rho n\pi d_i^4}$$

$$\Rightarrow \dot{W}_p = \frac{128\mu L}{n\pi d_i^4}\left(\frac{\dot{m}_H}{\rho}\right)^2 \tag{7}$$

where ρ is the gas density (kg/m^3) and μ is the dynamic viscosity (kg/ms). We shall write this as

$$\dot{W}_p = \frac{128\mu\dot{m}_H^2}{\rho^2\pi}\Omega \tag{8}$$

where Ω denotes the group L/nd_i^4.

We are going to propose a design made up of many short, narrow tubes. As we move toward such a design, a loss mechanism not previously important become significant—longitudinal thermal conduction through the tube metal from the hot end to the cool end. We denote the heat flow via this pathway by $\dot{W}_m$. Accurate calculation of this effect is difficult; a good treatment is provided by [7], pp. 4-53–4-56. For typical microtube heat exchanger designs, $\dot{W}_m$ is about 0.3% of the heat exchange power, so we introduce no serious inaccuracy by treating conduction losses through the tube material as decoupled from the flowing fluid:

$$\dot{W}_m \approx \frac{0.2n\pi d_i^2 k_m(T_H - T_C)}{L} = \frac{0.2\pi k_m(T_H - T_C)}{\Omega d^2} \tag{9}$$

where k_m is the tube metal conductivity, and T_H and T_C are the hot and cold temperatures, respectively. It is predominantly this loss mechanism that establishes the theoretical limit to specific conductance in high-efficiency counterflow exchangers.

Lastly, the condition that the internal flow be laminar is expressed by

$$\mathrm{Re} = \frac{4\dot{m}_h}{n\pi d_i\mu} \leq 2300 \tag{10}$$

Let us suppose that there is some combination of the parameters n, L, and d_i that gives a satisfactory value for effectiveness and gives acceptable levels of flow losses and conduction losses. We argue that, whatever the initial values are, it will always be possible to apply the following strategy: Reduce d_i by a factor p; simultaneously increase n and decrease L, each by a factor p^2, thus keeping flow losses and UA, hence ϵ, constant. This change will maintain laminar flow while reducing system mass by a factor p^2. We can reduce d_i until either conduction losses become unacceptable or until we go below the limits of manufacturability. The motivation for reducing d_i in this way is provided by Eq. (6): Mass, and hence, given our assumptions, cost, goes down as p^2.

We shall calculate a value of d_i typical of this design method. To compare losses via different mecha-

nisms, we shall nondimensionalize the losses by relating them to the ideal heat exchange power, that is, to the power required to change the temperature of the fluid stream with lesser thermal capacity by the amount ΔT, the temperature difference between hot and cold streams.

Let us suppose that for a given application, the pumping power may not exceed 1% of the ideal heat exchanger power. Then

$$\frac{\dot{W}_p}{\dot{m}c(T_H - T_C)} \leq 0.01 \tag{11}$$

Substituting from Eq. (8) and rearranging:

$$\Omega\dot{m} \leq \frac{\pi c(T_H - T_C)\rho^2}{12{,}800\mu} \tag{12}$$

Taking the maximum permitted value of $\Omega\dot{m}$ from Eq. (12), we consider the limit imposed by conduction losses. Let us also require that conduction losses not exceed 1% of the ideal heat exchange power. Then

$$\frac{\dot{W}_m}{\dot{m}c(T_H - T_C)} \leq 0.01 \tag{13}$$

Substituting from Eq. (9) and rearranging, then substituting from Eq. (12) gives

$$\Omega d_i^2 \dot{m} \geq \frac{20\pi k_m}{c}$$

$$\Rightarrow d_i^2 \geq \frac{20\pi k_m}{c\dot{m}\Omega}$$

$$\Rightarrow d_i \geq \sqrt{\frac{20 \times 12{,}800\mu k_m}{\rho^2 c^2 (T_H - T_C)}} \tag{14}$$

Evaluating Eq. (14) for a stainless steel heat exchanger with helium at 1 MPa as the working fluid, operating between temperatures of 900 and 300 K, we obtain a lower limit on tube diameter of about 90 μm. This figure is typical of the dimensions yielded by this design method, and is about an order of magnitude smaller than appears feasible from manufacturing and corrosion considerations. This establishes that, given our assumptions, it is desirable to design for the finest-diameter tubes feasible. (We have examined only tube-side flow, but a similar argument would lead to the same conclusions for shell-side flow.)

It may be questioned, however, whether our assumptions are reasonable. For some space applications, reducing heat exchanger mass is desirable in itself. To show that our technology is practical for terrestial applications, we must show that we can so reduce the cost of machining and assembly that material costs come to predominate; we must also address the problem of fouling and flow maldistribution. Before dealing with these questions, we shall fill out the above calculation with a complete design example, then describe an experimental test of the theory.

Let us suppose that the helium in the above example is flowing at 1 kg/s, and that we wish to exchange heat between this and another gas stream, flowing at the same rate, with an effectiveness of 95%. Substituting the appropriate values of physical constants in Eqs. (2), (4), and (5) and rearranging, we obtain

$$nL \geq 94{,}000 \text{ m} \tag{15}$$

We shall continue to require that the pumping power needed to overcome fluid friction be less than 1% of the heat exchange power. Using Eq. (7), we obtain

$$\frac{n}{L} \geq 100 \frac{128\mu}{\pi c(T_H - T_C)d_i^4} \left(\frac{\dot{m}}{\rho}\right)^2 \tag{16}$$

In accordance with our design strategy, we select the smallest value for d_i that it is practical to manufacture. We shall show below that this value is about 0.5 mm. Substituting for d_i and the other parameters, we obtain

$$\frac{n}{L} \geq 900{,}000 \tag{17}$$

Combining Eqs. (15) and (17) gives $L \approx 0.3$ m and $n \approx 300{,}000$. For very large-scale applications, the number of parallel tubes will be numbered in the millions, requiring thousands of parallel modules to maintain uniform shell-side flow (Fig. 2).

Such geometries are unusual for counterflow heat exchangers, but are quite typical of regenerative heat exchangers such as gas turbine rotating-porous-ceramic-wheel regenerators or Stirling-cycle wire-mesh regenerators.

Method of Manufacture

The discussion above assumes that manufacturing cost can be treated as primarily dependent on heat exchanger mass. As every heat exchanger designer knows, this is not currently the case. If our discussion of design is to be of more than academic interest, we

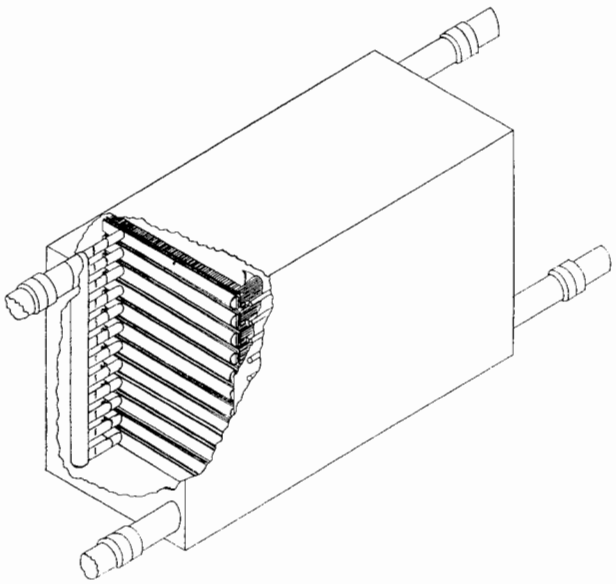

Figure 2 Bank of parallel MTS modules.

must therefore show that a practical method of manufacture can be found.

To realize the unconventional heat exchanger designs required by the above theory, we manifold together large numbers of identical modules, each module containing several hundred tubes. Each module is about 100 mm long; this length represents a compromise between the need to minimize conduction losses and the tendency of longer tubes to distort during the manufacturing process. The modules can be manifolded in series to achieve multiples of this length.

To facilitate uniform shell-side flow and to permit fineblanking of the header tubestrips, it is necessary to depart from the disk-shaped header tubesheet normally used in heat exchangers and use a rectangular header tubestrip, as shown, with fewer than 10 rows of tubes. Advances in high-speed laser welding technology and diamond dies make it possible to produce very small stainless steel tubing at low production costs—less than \$0.14 per meter [8]. These can be joined to the endplates by diffusion welding.

Advances in Diffusion Welding Technology

Diffusion welding occurs when clean metal surfaces are held together under pressure at high temperatures. The combined action of solid-state diffusion mechanisms and solid-state surface tension results in recrystallization or grain growth across an interface and the solution or dispersion of interfacial contaminants [9]. The time required to form the bond is an inverse exponential function of temperature and a quadratic function of surface finish and interfacial gaps [10]. For most nickel-chromium alloys with precision surfaces (0.4 μm rms) under moderate pressure (5 MPa, or 700 psi), high-quality welds (90% of the base metal strength) can be obtained in several seconds at 1230°C.

Method of Assembling Tube Arrays

We have developed a technique for joining microtubes to header strips *en masse*. The technique permits tube alignment, insertion, and welding rates to exceed 1,500,000 pieces per day per production line at an estimated production cost of less than \$0.01/tube. The following sequence of operations is followed: The tubes are finished to the required length; the tubes are inserted into adjacent, parallel, precision, nonsacrificial space forms, similar in size and pattern to the header tubestrips but with precision, slip-fit, countersunk holes (Fig. 3a), using a hopper-and-Gatling-gun arrangement (Fig. 3b). Next, the spacer forms are slid apart to near opposite ends of the tubes; caps are placed over the ends of the tube to secure the tube ends (Fig. 3c), and the tuber-spacer-cap fixture assembly is placed in a mold suitable for vacuum injection (Fig. 3d). The mold is evacuated and a molten, fusible alloy is injected into the heated mold. The mold is then cooled below the solidus temperature, the encapsulated assembly removed, and the securing caps and spacer forms slid off, exposing the tube ends (Fig. 3e). Lastly, the assembly is loaded into a suitable fixture on a press and the header tubestrips pressed onto opposite ends of the tubes (Fig. 3f; the typical force required for 1000 1-mm tubes is 10^5 N, about 10 tons). The fusible alloy is melted and cleaned from the assembly by a combination of melting, vibration, and air jets, followed by chemical cleaning.

Suitable weld conditions are readily achieved if the tube diameter and hole size can be held to very tight tolerances. The use of hardened tubes and annealed tubestrips then makes it possible to press the tubes into slightly undersized holes in the thin, rectangular, header tubestrip. With hard, straight tubes, of length less than 300 times their OD, it is possible to press them into soft tubestrips with up to 3% interference without serious difficulty. With proper attention to surface quality and a minimum of 0.4% interference fit, the conditions required for diffusion welds are readily achieved. Surface finishes of about 0.4 μm rms in the area of the diffusion weld have proven to be 100% leak-tight—within 10^{-6} standard mm^3/s to hydrogen at 1 atm.

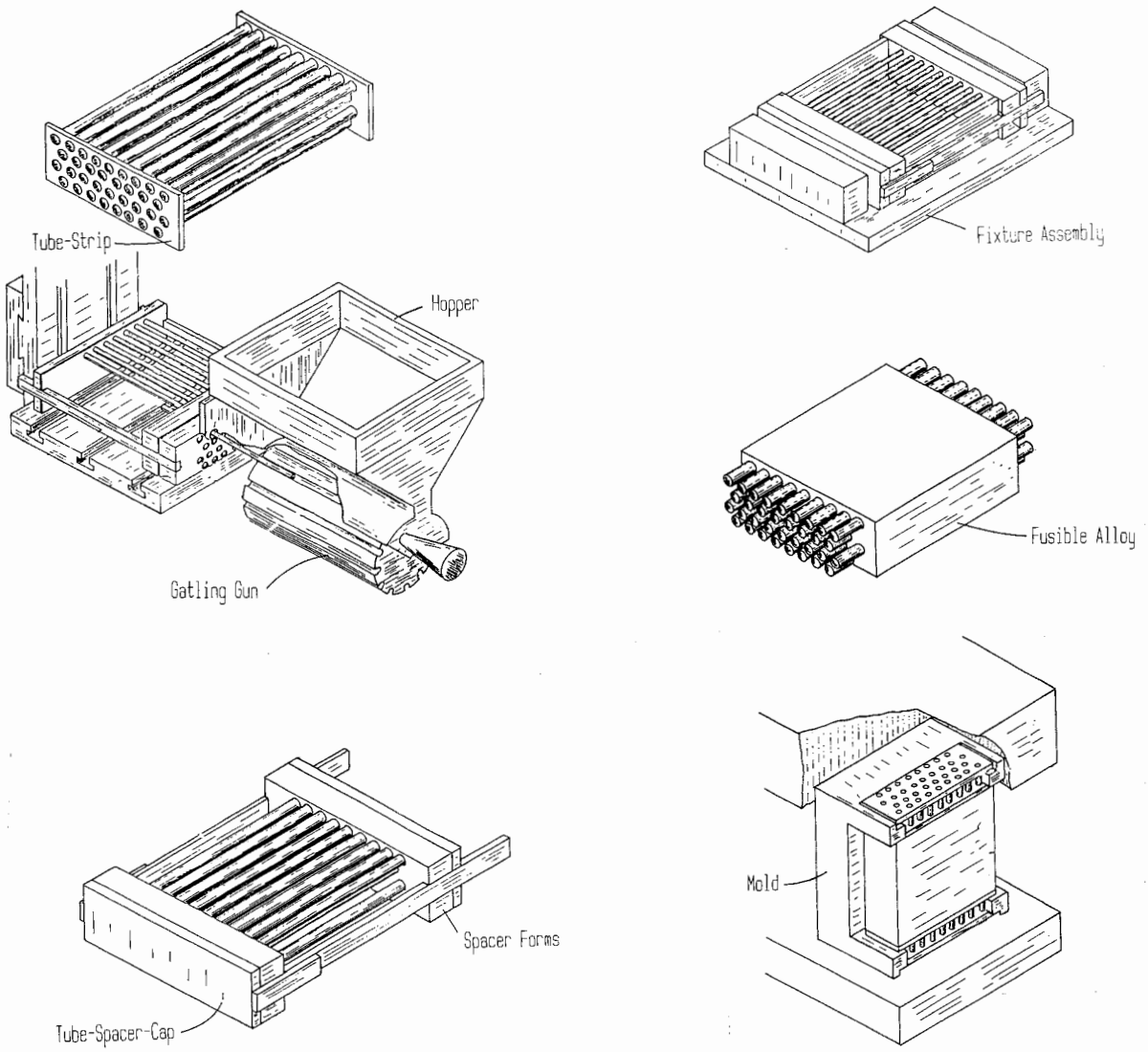

Figure 3 Method of assembly.

After the header tubestrips have been pressed onto the microtubes and the assembly of microtubes and header tubestrips is thoroughly cleaned, it must be heated to effect the diffusion weld to the tubes. Most of our diffusion welding thus far has been done in inert or reducing atmosphere ovens and consequently has been limited to slow cycles. Numerous experiments are required to determine optimum surface preparation techniques, atmosphere, interference, and temperature cycle for diffusion welding. About 10 s at 1230°C appears sufficient for full-strength diffusion welds in the Ni-Cr-W superalloy Haynes 230.

Advances in Finebanking Technology

The requirement of low production costs in the hard-drawn 1-mm tubing imposes a tolerance limit of $\pm 0.4\%$, which then leaves a $\pm 0.9\%$ tolerance requirement for the hole diameters in the tubestrip. Fortunately, the hole diameter need not be constant over the majority of its length, and a slight taper is in fact beneficial in assembly. Punching consistently suitable, closely spaced microholes in superalloys does represent a major technical challenge. Our initial prototypes used drilled holes, followed by reaming. More recently, we have successfully used tubestrips produced by Swiss fineblanking—a controlled cold-flow blanking (punching) process that includes the use of a counterpunch and a high-pressure ring indenter (stripper), which applies sufficient pressure to the metal surfaces near the punch edges to prevent normal and planar deformation of the material during punching [11]. The technique requires compound dies and triple-action presses, but results in minimal edge fracturing and deformation.

No other technique can come close to competing

on a cost basis in large-scale production with Swiss fineblanking—less than $1 per tubestrip. However, electrochemical and electrical discharge techniques are likely to permit even smaller holes with closer spacing. We also plan to evaluate these techniques—especially for small-scale, ultrahigh-density applications.

EXPERIMENTAL RESULTS

We have assembled several dozen fully welded prototype 103-tube MTS modules similar to the one shown in Fig. 1. The modules used 0.33-mm-ID tubes, 127 mm in length, with 0.1524-mm walls. The tubestrip has five rows of tubes with 21 holes in the odd-numbered rows and 20 holes in the even-numbered rows, arranged in a triangular pitch on 1.25-mm centers. Three modules were assembled into shells with manifolds to distribute tube-side and shell-side flows, and baffles between the modules to promote uniform shell-side flow through each module.

Figure 4 shows a finished prototype bank. The entire assembly has an overall length of 190 mm, a height of 30 mm, a width of 35 mm, and a total mass of 0.3 kg. Scaling up to a bank with greater numbers of modules and more tubes per module would reduce the specific mass of the bank by up to 70%.

The finished bank was used for gas–gas heat exchange, using the experimental setup diagrammed in Fig. 5. High-pressure gas from a bottled supply was supplied to the tube side, its inlet and outlet temperatures, T_3 and T_4, being measured using sheathed and grounded 1.6-mm Type 4 chromel-alumel thermocouples. The outlet gas was then expanded through a pressure-reduction valve, electrically heated, and allowed to flow through the shell side, inlet and outlet temperatures T_1 and T_2 again being measured with unshielded chromel-alumel thermocouples. The outlet gas was exhausted to atmospheric pressure, its volumetric flow rate being measured with a Dwyer floating-ball flowmeter. Pressure drops across tube

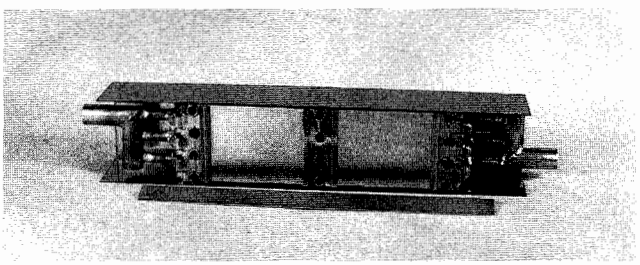

Figure 4 Three-module prototype bank.

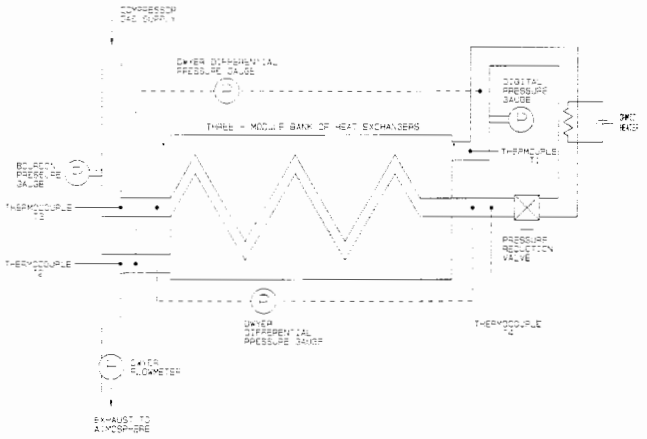

Figure 5 Experimental setup.

side and shell side were measured using Dwyer differential pressure transducers. Following each change in gas flow rate, care was taken to ensure that flowmeter and thermocouple readings reached steady values before any measurements were taken.

Data Reduction

To compare the experimental results with our theoretical analysis, we calculate the effectiveness of the heat exchanger from the temperature measurements T_1, T_3, and T_4. Since the thermal capacities of the hot and cold streams are equal, we can invert Eq. (4) to calculate NTU from effectiveness:

$$\text{NTU} = \frac{\epsilon}{1 - \epsilon} \tag{18}$$

We calculate UA from

$$UA = \frac{\dot{m} c_p \, \Delta T}{T_\delta} \tag{19}$$

where ΔT is the temperature drop between T_1 and T_2 and T_δ is the mean temperature difference between hot and cold streams. We compare this with the value predicted by our Eq. (5), using tabulated values for k_C and k_H, evaluated at the mean tube-side and shell-side temperatures, respectively. Similarly, we compare measured values of Δp with those calculated from Eq. (7). The errors for each calculated quantity are estimated using Theorem 3 from [12]. The most serious source of error arises from the small values of T_δ at high effectiveness; this may be remedied by the use of differential thermocouples.

The values of UA calculated from Eq. (5) are ob-

Table 1 Experimental and Predicted Heat Transfer

$\dot{m}$ (mg/s)	p (kPa)	T_1 (C)	T_2 (C)	T_3 (C)	T_4 (C)	ϵ (%)	NTU	UA (W/K)	UA [Eq. (5)]
Nitrogen									
470 ± 20	322 ± 3	104.7 ± 0.5	30.9 ± 0.5	23.0 ± 0.5	93.0 ± 0.5	85.7 ± 0.6	6.0 ± 0.3	3.7 ± 0.4	7.1
840 ± 20	322 ± 3	96.5 ± 0.5	32.3 ± 0.4	23.3 ± 0.5	84.1 ± 0.5	83.1 ± 0.7	4.9 ± 0.2	5.3 ± 0.5	7.1
930 ± 20	322 ± 3	99.4 ± 0.5	33.0 ± 0.5	22.8 ± 0.5	85.8 ± 0.5	8.2 ± 0.7	4.6 ± 0.2	5.4 ± 0.5	7.1
373 ± 20	705 ± 3	51.4 ± 0.5	28.5 ± 0.5	26.1 ± 0.5	48.8 ± 0.5	89.7 ± 0.7	8.7 ± 0.6	3.5 ± 1.4	7.1
738 ± 20	1462 ± 3	64.7 ± 0.5	28.9 ± 0.5	25.3 ± 0.5	59.2 ± 0.5	86.0 ± 0.7	6.1 ± 0.4	6.0 ± 1.3	7.1
1085 ± 20	1068 ± 3	64.8 ± 0.5	28.6 ± 0.5	23.6 ± 0.5	58.3 ± 0.5	84.2 ± 0.7	5.3 ± 0.3	7.1 ± 1.2	7.1
1413 ± 20	1486 ± 3	67.3 ± 0.5	29.3 ± 0.5	22.9 ± 0.5	59.5 ± 0.5	82.4 ± 0.7	4.7 ± 0.2	7.9 ± 1.1	7.1
1824 ± 20	1470 ± 3	58.1 ± 0.5	23.3 ± 0.5	15.3 ± 0.5	48.8 ± 0.5	78.2 ± 0.7	3.6 ± 0.1	7.6 ± 0.9	7.1
Helium									
117 ± 7	749 ± 3	107.5 ± 0.5	28.3 ± 0.5	23.5 ± 0.5	103.6 ± 0.5	95.4 ± 0.6	21 ± 3	11.1 ± 2.5	39.0
79 ± 7	756 ± 3	103.8 ± 0.5	29.5 ± 0.5	24.0 ± 0.5	100.5 ± 0.5	95.7 ± 0.7	22 ± 4	6.9 ± 1.6	39.0
213 ± 7	825 ± 3	109.4 ± 0.5	28.7 ± 0.5	23.1 ± 0.5	103.4 ± 0.5	93.0 ± 0.7	13.3 ± 1.4	15.4 ± 2.6	39.0

tained setting the dimensionless parameters a and b to unity and are tabulated in Table 1. These calculated values agree quite well with the experimental results for moderate values of effectiveness (75–85%). At higher values of ϵ, however, there is clearly a discrepancy between theory and experiment, which we believe to result from flow maldistribution. In support of this belief, we note that the discrepancy is most serious at low flow rates, consistent with the findings of Mueller and Chiou [13].

The increase in UA with flow rate might be attributed to turbulence, but we think this unlikely: The maximum tube-side Reynolds number was approximately 1400 for nitrogen, 160 for helium. Turbulence would also be expected to result in measured values of Δp higher than predicted by Eq. (7).

Tube-side pressure drops were also measured, and are reported in Table 2. These results are reasonably well predicted, though experimental results for helium are somewhat lower than expected. This is consistent with minor tube-side maldistribution, though we expect the major maldistribution problems to be on the shell side.

Even given the extent to which measured heat transfer falls short of theoretical performance at high ϵ, the absolute values of specific conductance demonstrated are quite encouraging, with a figure of 50 W/K kg for the sixth test.

OPERATIONAL PROBLEMS

We have argued that a laminar-flow design is theoretically appealing, and reported some experience with the manufacture of a prototype. Several major questions, however, must be addressed before heat exchangers of the MTS type can be considered for practical use.

Fouling

Fouling is often a serious problem for heat exchanger designs characterized by very narrow flow passages, as is the MTS heat exchanger. Marner and Suitor point out in their review of this area that fouling exacts a double penalty, reducing effectiveness and increasing pressure drop [14]. In the laminar-flow regime, if the fouling is uniform between tubes and the conductivity of the deposit is high compared with that of the working fluid, Eq. (5) suggests that the effectiveness penalty will not be serious. There are some applications in which fouling is unlikely to be of concern, for example, gas–gas heat exchange in a closed Brayton cycle used for extracting power

Table 2 Experimental and Predicted Pressure Drop

$\dot{m}$ (mg/s)	p (KPa)	Δp (kPa)	Δp [Eq. (7)]
Nitrogen			
470 ± 20	322 ± 3	5.1 ± 0.2	3.7 ± 0.2
840 ± 20	322 ± 3	9.5 ± 0.2	6.6 ± 0.2
930 ± 20	322 ± 3	11.1 ± 0.2	7.3 ± 0.2
373 ± 20	705 ± 3	1.3 ± 0.05	1.3 ± 0.2
738 ± 20	1462 ± 3	1.5 ± 0.05	1.3 ± 0.2
1084 ± 20	1068 ± 3	3.3 ± 0.1	2.5 ± 0.2
1413 ± 20	1486 ± 3	3.7 ± 0.1	2.3 ± 0.2
1824 ± 20	1470 ± 3	5.5 ± 0.2	3.1 ± 0.2
Helium			
117 ± 7	749 ± 3	2.3 ± 0.1	3.0 ± 0.2
79 ± 7	756 ± 3	1.5 ± 0.05	2.0 ± 0.2
213 ± 7	825 ± 3	4.4 ± 0.1	5.5 ± 0.2

from a nuclear reactor, and for these applications the MTS heat exchanger may be appealing. For other applications, it may be possible to reduce fouling to acceptable levels by continuous cleaning of the gas streams. We are in the process of evaluating several cleaning methods, including filtration and electrostatic precipitation [15].

Flow Maldistribution

The very small scale of the component modules of the MTS heat exchanger requires careful design of manifolds and baffles if flow maldistribution is not be a problem. Mueller and Chiou give a general review of this problem in [13]. Of the causes of flow maldistribution discussed in [13], poor manufacturing tolerances are not thought to be a problem for tube-side flow at the level of individual MTS modules: The method of manufacture gives a very uniform tube size. As the experimental results suggest, however, shell-side maldistribution does appear to be a serious problem in the prototype banks. We are currently investigating the extent and control of shell-side flow maldistribution, and the optimal design of manifolds and baffles.

In addition to irregularities in heat exchanger construction, flow maldistribution in laminar-flow heat exchangers may also arise from temperature-dependent variations in fluid viscosity. This is discussed by Putnam and Rohsenow in [16]. How seriously this will affect performance must be determined by calculation for each application being considered.

Applications

The most attractive short-term applications for the MTS technology are those where minimizing specific conductance is important, and where fouling factors are low. The first consideration suggests space-power applications, the second suggests closed-cycle applications.

Surface Cooling

There are applications where it is necessary to handle extremely high surface heat fluxes (the first wall in a fusion reactor [17], rocket nozzle and diffuser cooling, etc.). The MTS principles may be readily adapted to extreme surface thermal management by encasing the microtube portion of the module in solid, high-conductivity metal, as shown in Fig. 6.

Some specific aerospace applications that we are addressing with this technology include (1) cooling of leading edges of wings of hypersonic aircraft, (2) cooling of fuel-injector struts in scram-jet engines, (3) low-temperature remote surface heat rejection, (4) cabin environment conditioning, and (5) electronic-instrument power dissipation.

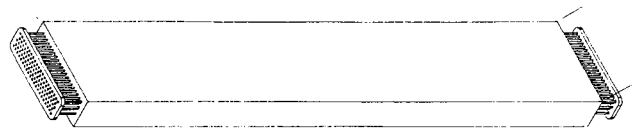

Figure 6 Surface heat exchanger.

Heat Engines

External combustion engines, such as the Stirling engine and the closed Brayton cycle engine [18], have received increased attention in recent years owing to their multifuel capability and their potential for reducing emissions. Among the obstacles to the wider use of these engines has been their requirement for large, expensive heat exchangers. In the Stirling engine, the internal volume of the heat exchangers carries an additional penalty, as it reduces the specific power of the engine [19]. This is a suitable application for the MTS heat exchanger. Tube-side fouling is not expected to be a problem, as the working fluid is typically a fixed mass of high-pressure gas, such as helium or hydrogen. Shell-side fouling by combustion products may present problems, but the use of a heat pipe in combination with the heat exchanger is a proven alternative [19].

Cryogenic Cooling

The MTS exchanger can be used for cooling of helium in the temperature range 4–80 K. The chief problems here are fouling by the freezing-out of other gases that may be present, and the possibility of viscosity-induced flow maldistribution [16]. Further research is needed to determine the severity of these problems and suitable methods for avoiding them.

CONCLUSION

We have presented arguments to show that, if we take advantage of the unconventional heat exchanger design options made possible by modern manufacturing techniques, we can achieve specific conductances comparing favorably with the best current shell-and-tube exchangers. These high-performance heat exchangers operate in the laminar-flow regime, and

thus have low pumping losses and very low levels of vibration, resulting in reduced operating costs and longer life. We have described the manufacturing process in some detail, and identified the questions requiring further research.

Experiments on a prototype heat exchanger bank have shown that performance agrees reasonably well with calculation at levels of effectiveness in the range 75–85%, but falls seriously short of predicted values at higher effectiveness. We have given reasons for thinking that this is due to shell-side flow maldistribution. Performance may be improved by using several banks in series, with mixing stations between successive banks; research is needed into this and other ways of improving distribution. Even at the lower levels of effectiveness, the specific conductance of the heat exchanger compares favorably with current practice; we therefore believe that this approach to heat exchanger design deserves continued attention.

Lastly, we have mentioned several potential markets for the new technology.

NOMENCLATURE

a, b	dimensionless constants near unity, dependent on exchanger geometry
A	total heat exchanger area, m^2
c	specific heat of gas, J/kg K
c_C	specific heat of the cooler gas, J/kg K
c_H	specific heat of the hotter gas, J/kg K
c_{max}	specific heat of gas with greater heat capacity, J/kg K
c_{min}	specific heat of gas with lesser heat capacity, J/kg K
d_i	heat exchanger tube inner diameter, m
d_o	heat exchanger tube outer diameter, m
k	conductivity, W/m K
k_C	conductivity of the cooler gas, W/m K
k_H	conductivity of the hotter gas, W/m K
k_m	conductivity of tube material, W/m K
L	length of tubes in heat exchanger, m
M	mass of heat exchanger, kg
$\dot{m}$	gas mass flow rate, kg/s
$\dot{m}_C$	mass flow rate of cooler gas, kg/s
$\dot{m}_H$	mass flow rate of hotter gas, kg/s
$\dot{m}_{max}$	mass flow rate of gas with greater heat capacity, kg/s
$\dot{m}_{min}$	mass flow rate of gas with lesser heat capacity, kg/s
n	number of tubes in heat exchanger
NTU	number of transfer units [See Eq. (2)]
p	dimensionless scaling factor
R	ratio of heat capacities of the two fluid streams
Re	Reynolds number (ratio of turbulent to viscous forces)
T_C	temperature at cold end of exchanger, K
T_H	temperature at hot end of exchanger, K
U	effective heat transfer coefficient, W/m^2 K
w	tube wall thickness, m
$\dot{W}_m$	thermal conduction loss along exchanger, W
$\dot{W}_p$	tube-side pumping power loss, W
ϵ	heat-exchanger effectiveness
μ	gas viscosity, kg/m s
ρ	gas density, kg/m^3
ρ_m	density of tube material, kg/m^3
Ω	the group (L/nd^4), m^{-3}

REFERENCES

[1] Bejan, A., *Adv. Heat Transfer,* vol. 15, p. 1, 1982.

[2] Apblett, W. R. (ed.), *Shell and Tube Heat Exchangers,* ASM, Metals Park, Ohio, 1962.

[3] Wilson, D. G., *The Design of High-Efficiency Turbomachinery and Gas Turbines,* MIT Press, Cambridge, Mass., 1984.

[4] Hsu, S. T., *Engineering Heat Transfer,* Van Nostrand, Princeton, N.J., 1963.

[5] Bejan, A. *Convective Heat Transfer,* John Wiley, New York, 1984.

[6] Shapiro, A. H., *Compressible Fluid Flow,* vol. I, John Wiley, New York, 1953.

[7] Shah, R. K., Compact Heat Exchangers, in *Handbook of Heat Transfer Applications,* 2nd ed. (W. M. Rohsenow, J. P. Hartnett, and E. N. Ganic, eds.), chap. 4, part III, pp. 4-174–4-311, McGraw-Hill, New York, 1985.

[8] Dickenson, J., K-Tube, San Diego, Calif., 1988 (personal communication).

[9] Schwartz, M. M., *Metals Joining Manual,* McGraw-Hill, New York, 1979.

[10] Bradley, E. F. (ed.), *Source Book on Materials for Elevated Temperature Applications,* ASM, Metals Park, Ohio, 1979.

[11] Lange, K., Ed., *Handbook of Metal Forming,* McGraw-Hill, New York, 1985.

[12] Kline, J. S., and McClintock, F. A., Describing Uncertainties in Single-Sample Experiments, *Mech. Eng.,* pp. 3–8, January 1953.

[13] Mueller, A. C., and Chiou, J. P., Review of Various Types of Flow Maldistribution in Heat Exchangers, *Heat Transfer Eng.,* vol. 9, no. 2, pp. 36–49, 1988.

[14] Marner, W. J., and Suitor, J. W., Fouling with Convective Heat Transfer, in *Handbook of Single-Phase Convective Heat Transfer* (S. Kakac, R. K. Shah, and W. Aung, eds.), chap. 21, John Wiley, New York, 1987.

[15] Doty, F. D., Jones, J. D., and Helms, R., The MTS Heat Exchanger/The Doty Engine, Doty Scientific, Columbia, S.C., 1989.

[16] Putnam, G. R., and Rohsenow, W. M., Viscosity-Induced Non-Uniform Flow in Laminar Flow Heat Exchangers, *Int. J. Heat Mass Transfer,* vol. 28, pp. 1031–1038, 1985.

[17] Stacey, W. M., Jr., *Fusion, An Introduction to the Physics*

and Technology of Magnetic Confinement Fusion, John Wiley, New York, 1984.

[18] Doty, F. D., and Jones, J. D., A New Look at the Closed Brayton Cycle, Paper 900166, Proc. 1990 IECEC Conf., Reno, Nevada, August 12–17, 1990.

[19] Walker, G., *Stirling Cycle Machines*, Oxford University Press, Oxford, UK, 1980.

John Dewey Jones is an associate professor in the School of Engineering Science, Simon Fraser University, British Columbia. He received his Ph.D. in engineering from the University of Reading (UK) in 1983, and subsequently worked for five years at General Motors Research Laboratories, Michigan. His research interests are in the areas of heat transfer, thermodynamics, and the use of artificial intelligence in engineering design. He is a registered professional engineer in the state of Michigan.

David Doty received his Ph.D. in physics from the University of South Carolina in 1983. Since that time he has been the president of Doty Scientific, Inc.; his company originally concentrated on the manufacture of NMR equipment, but has since diversified into heat exchange equipment and specialized turbomachinery. Dr. Doty's research interests include nuclear magnetic resonance, heat exchanger design, and turbine and compressor design. He holds 10 U.S. patents for innovations in these and other fields.

Greg Hosford graduated from Brigham Young University with a B.S.M.E. in 1976, and with an M.S.M.E. in 1977. Since then he as worked as an engineer for John Deere, where he analyzed production/reliability issues in environmental systems, and as a senior research engineer for Sundstrand Corporation, where he worked on integrated power/thermal management system design for advanced aerospace power generation. He has been project engineer in charge of MTS heat exchangers at Doty Scientific since 1988.

J. B. Spitzmesser is vice-president in charge of manufacturing at Doty Scientific, Inc. He has been working for DSI since 1982, and has helped to develop the manufacturing techniques used to produce the microtube strip heat exchanger. He holds two patents connected with novel heat exchanger designs, and has extensive experience in a range of manufacturing and machining technologies.